Applied Surface Science 447 (2018) 325–330

Contents lists available at ScienceDirect

Applied Surface Science

journal homepage: www.elsevier.com/locate/apsusc

Full Length Article

Humidity sensing properties of the hydrothermally synthesized WS_2-modified SnO_2 hybrid nanocomposite

Yunpeng Chen [1], Yongyong Pei [1], Zimin Jiang, Zhifeng Shi, Junmin Xu, Di Wu, Tingting Xu *, Yongtao Tian, Xinchang Wang, Xinjian Li *

Department of Physics and Engineering, Key Laboratory of Material Physics, Zhengzhou University, Zhengzhou 450052, PR China

ARTICLE INFO

Article history:
Received 14 September 2017
Revised 18 March 2018
Accepted 20 March 2018
Available online 27 March 2018

Keywords:
Hybrid nanocomposite
Hydrothermal
Humidity
Response

ABSTRACT

WS_2-modified SnO_2 hybrid nanocomposite was synthesized by a hydrothermal method. The morphology and structure characterization revealed that the SnO_2 nanocrystals were anchored to the WS_2 nanosheets in the homogeneous nanocomposites. The resistive humidity sensors based as-prepared nanocomposites, pure WS_2 nanosheets and pure SnO_2 microspheres were fabricated and tested in a humidity range of 11–95% RH at 25 °C. The humidity sensing properties of the nanocomposites manifested a good and stable humidity sensing. The response of the hybrid nanocomposite in air with 95% RH was found to be 8.5 and 862.8 times higher than that of pure SnO_2 microspheres and WS_2 nanosheets, respectively. The synergistic effect between WS_2 and SnO_2 played an important role in improving the humidity sensing performance of the hybrid nanocomposites.

1. Introduction

In order to meet the demand for humidity detection in industrial productions, food storage and environment monitoring, great efforts have been made to explore humidity-sensitive materials for the fabrication of high-performance humidity sensors. Until now, various functional materials have been utilized as humidity sensing materials, such as metal oxides [1–2], carbon nanomaterials [3] and hybrids composites [4–5]. SnO_2 is an important n-type semiconductor for humidity detection [1]. Since it was reported that the single-crystalline SnO_2 nanowires exhibited a fast and high response to RH changes at 30 °C [6], SnO_2-based nanostructures have been attracting more and more interests due to their high chemical stability, wide operating temperature range, non-toxicity and low-cost [7]. However, the sensitivity and response/recovery time of the humidity sensors based on SnO_2 nanostructures have impeded their practical applications.

Recent research has proved that decorating SnO_2 nanostructures with other materials is an effective route to enhance their humidity sensing properties. The sensitivity of the humidity sensor increased by 5.5 times after the SnO_2 nanostructures were decorated with Ag nanoparticles [8]. The Li^+-doped SnO_2 porous nanofibers obtained an ultrafast response and achieved a 15 times higher response than that of pristine SnO_2 porous nanofibers at 85% RH [9]. The humidity sensing properties of NiO-SnO_2 nanofibers were investigated [10]. In additional to metal and metal oxide, the humidity sensing properties of SnO_2 nanostructures decorating with two-dimensional (2D) materials (such as graphene and MoS_2) were also explored. Because of the high surface-to-volume ratio of 2D materials [11–12], the decorated SnO_2 nanostructures demonstrated excellent humidity sensing properties. It was found that the reduced graphene oxide-SnO_2 (rGO-SnO_2) nanocomposites have a better sensitivity factor and faster response and recovery times compared to SnO_2 zigzag belts [13] and nanowires [6]. The humidity response of MoS_2-SnO_2 hybrid reached up to 32,850 and increased by 1.5 times compared to that of pure SnO_2 [14]. As the same as MoS_2, WS_2 is an important 2D metal dichalcogenide, and has exhibited obvious responses to NO_2, NO, NH_3 at 25 °C [15–16], indicating that WS_2 has great potential for gas and humidity detection. Herein, WS_2-modified SnO_2 hybrid nanocomposite was prepared by a hydrothermal method, and its crystallinity, morphology and structure were investigated by X-ray diffraction (XRD), field emission scanning electron microscopy (FESEM), transmission electron microscopy (TEM) and energy dispersive X-ray spectrometry (EDS), respectively. The resistant humidity sensors based as-prepared nanocomposites, pure WS_2 nanosheets, and pure SnO_2 were fabricated and tested in a humidity range of 11–95% RH at 25 °C. The humidity sensing properties of the nanocomposites manifested a good and stability humidity sensing. The response of the nanocomposite was found to be

* Corresponding authors.
E-mail addresses: xutt@zzu.edu.cn (T. Xu), lixj@zzu.edu.cn (X. Li).
[1] Equal contrubutions to the work.

https://doi.org/10.1016/j.apsusc.2018.03.154
0169-4332/

8.5 and 862.8 times higher than that of SnO_2 microspheres and WS_2 nanosheets at 95% RH, respectively.

2. Experimental

2.1. Materials synthesis

The synthesis of the WS_2-modified SnO_2 hybrid nanocomposite consists of the prior preparation of WS_2 nanosheets and the following synthesis of WS_2-modified SnO_2. In the preparation process of WS_2 nanosheets, high purity sodium tungstate ($Na_2WO_4{\cdot}2H_2O$, 99.9%, 1.5 mmol) and Cetyltrimethyl ammonium bromide (CTAB, 99.9%, 2.7 mmol) were dissolved in deionized water, and the pH of the solution was adjusted to the range of 2–3 by the addition of diluted hydrochloric acid (2 mol/L). The suspension was placed in a Teflon-lined stainless steel autoclave and the temperature was kept at 180 °C in a drying oven for 48 h. The resulting suspension was centrifuged and washed with ethanol for several times and then dried in a vacuum drying oven at 80 °C for 8 h. WS_2 nanosheets were obtained after the sulfurization of the primary product at 800 °C at the down stream of sulfur powder in a tube furnace. The obtained WS_2 nanosheets (40 mmol/L), $SnCl_4{\cdot}5H_2O$ (70 mmol/L) and NaOH (0.5 mol/L) were dissolved in deionized water and stirred for 0.5 h. Hydrothermal treatment of the above-mentioned solutions was performed at 180 °C for 48 h. Finally, WS_2-modified SnO_2 hybrid nanocomposites were obtained after the ordinary washing and drying process as mentioned above. What's more, in order to compare the humidity sensing properties between pure SnO_2 and WS_2-modified SnO_2 hybrid nanocomposites, SnO_2 microspheres were obtained with $SnCl_4{\cdot}5H_2O$ (70 mmol/L) and NaOH (0.5 mol/L), and the preparation conditions were same with that of WS_2-modified SnO_2 hybrid nanocomposites.

The as-prepared WS_2 nanosheets, SnO_2 microspheres and WS_2-modified SnO_2 hybrid nanocomposites were characterized by XRD with Cu Kα radiation (PA National X′ Pert Pro) and FESEM (JEOL, JSM-6700F). The SnO_2 microspheres and WS_2-modified SnO_2 hybrid nanocomposites were further characterized by TEM (JEOL, JEM-2100) and EDS.

2.2. Fabrication and testing of the resistive humidity sensors

Resistive humidity sensors were fabricated based on the commercial alumina ceramic substrates fixed with interdigital silver electrodes on the top surface. The as-prepared WS_2-modified SnO_2 hybrid nanocomposites were dispersed on the interdigital silver electrodes by brush coating. Each microelectrode in the interdigital silver electrodes was 0.2 mm in width and 5.6 mm in length, and the distance between adjacent microelectrodes were 1 mm. The working area of the humidity sensor was about 7 mm × 7.4 mm in size. The humidity sensing properties of as-fabricated resistive humidity sensors were investigated by exposing the sensors to different RH levels at 25 °C. The saturated salt solutions of LiCl, $MgCl_2$, $Mg(NO_3)_2$, NaCl, KCl and KNO_3 were used to yield 11, 33, 54, 75, 85, 95% RH levels, respectively.

3. Results and discussion

3.1. Materials characterizations

The crystallographic structure and phase purity of the as-fabricated WS_2 nanosheets, WS_2-modified SnO_2 hybrid nanocomposites and SnO_2 microspheres were revealed by the XRD pattern in Fig. 1. All the diffraction peaks of the WS_2 nanosheets and SnO_2 microspheres were well ascribed to the hexagonal WS_2

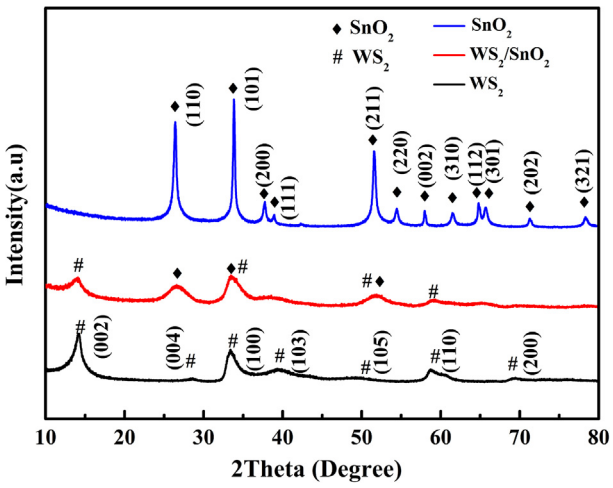

Fig. 1. XRD pattern of the as-prepared WS_2 nanosheets, WS_2-modified SnO_2 hybrid nanocomposites and SnO_2 microspheres.

(JCPDS-ICDD 84-1398) and tetragonal SnO_2 (JCPDS-ICDD 77-0451), respectively. The diffraction peaks of WS_2-modified SnO_2 hybrid nanocomposites at 27°, 14° and 59° were accurately indexed to the (1 1 0) plane of tetragonal SnO_2, (0 0 2) and (1 1 0) planes of hexagonal MoS_2, respectively. Since several diffraction peak positions of tetragonal SnO_2 and hexagonal MoS_2 are very close with each other, tetragonal SnO_2 and hexagonal MoS_2 both contributed to the diffraction peaks around 33° and 52°, resulting in the broadening FWHM (full width at half maximum) of the two diffraction peaks. All the diffraction peaks of the WS_2-modified SnO_2 hybrid nanocomposites corresponded to the presence of MoS_2 and SnO_2 crystals, illustrating the successful preparation of the nanocomposite.

The typical morphologies of as-prepared WS_2 nanosheets and WS_2-modified SnO_2 hybrid nanocomposites were demonstrated by SEM, as shown in Fig. 2a–b. As reported in the previous work [17], the WS_2 nanosheets were ultra-thin and possessed a three dimensional wall-like structures. In the WS_2-modified SnO_2 hybrid nanocomposites, there were nanocrystals uniformly attached to the surface of WS_2 nanosheets. The High resolution TEM image in Fig. 2c revealed that the SnO_2 nanocrystals were anchored to the WS_2 nanosheets. The lattice spacings of 0.26 nm and 0.34 nm corresponded to the (1 0 1) and (1 1 0) planes of tetragonal SnO_2, respectively. A layered structure with a lattice spacing of 0.62 nm was recognized as hexagonal WS_2. The selected area electron diffraction (SAED) pattern of the hybrid nanocomposites were shown in Fig. 2d, and the disperse rings in the SAED pattern were well indexed to the crystal planes of tetragonal SnO_2 or hexagonal WS_2. Because several lattice spacings of tetragonal SnO_2 and hexagonal WS_2 are approximately equal to each other, the corresponding disperse rings of them appeared to overlap, which is consistent with the XRD pattern in Fig. 1. The corresponding crystal planes of tetragonal SnO_2 and hexagonal WS_2 were both marked in Fig. 2d. The disperse rings in the SAED pattern were well indexed to the crystal planes of SnO_2 (1 1 0), WS_2 (1 0 0)/SnO_2 (1 0 1), WS_2 (1 0 3)/SnO_2 (1 1 1), WS_2 (1 0 5)/SnO_2 (2 1 1), WS_2 (1 0 7)/SnO_2 (3 1 0), SnO_2 (3 3 0), respectively. What's more, the HRTEM image in Figs. 2c and S1c revealed that the SnO_2 grain size in the hybrid nanocomposites was smaller than that in pure SnO_2. As a result, the broadening diffraction peak corresponding to (1 1 0) plane of tetragonal SnO_2 in the XRD pattern of the hybrid nanocomposites can be attributed to the grain refinement.

In order to explore the distribution of SnO_2 and WS_2 in the WS_2-modified SnO_2 hybrid nanocomposites, the scanning